**Proceedings of the 17th World Congress**
**The International Federation of Automatic Control**
**Seoul, Korea, July 6-11, 2008**

# Vision-based determination of wheel camber angle and tire deflection

**C. Lamy** [*,**] **M. Basset** [*]

[*] *Laboratory MIPS, Université de Haute - Alsace*
*12 rue des Frères Lumière 68100 MULHOUSE*
*(e-mail: christophe.lamy@uha.fr, michel.basset@uha.fr).*
[**] *Renault s.a.s. - DREAM / DTAA*
*Centre Technique d'Aubevoye, Le Parc de Gaillon 27940 AUBEVOYE*
*(e-mail: christophe.lamy@renault.com).*

**Abstract:** Accurate determination of vehicle's lateral behavior is necessary in the domain of vehicle dynamics and more particularly in the context of improvement of vehicle safety. Thus, a cutting-edge knowledge of its interaction with the road surface is primordial. In consequence, the integration of a force model, representing the tire/ground interface, into the global vehicle model is needed. The validity of such a model directly depends on its nature and more particularly on the determination accuracy of its inputs and outputs. This paper focalizes on an input: the wheel/road camber angle. Studies in collaboration with a carmaker have shown a required measurement accuracy lower than $\pm 0.1^\circ$ in order to identify the tire model parameters from real data with a high precision. Different existing solutions were studied and their accuracy was estimated. In parallel, a new method for direct camber determination was developed in the laboratory. Its vision-based principle's major purpose is to give an accurate measurement: its precision is robust to the road unevenness and the vehicle's velocity. The tire deflection is estimated in the same time. The method feasibility and its measurement precision were studied from real tests with the laboratory test car.

Keywords: Vehicle dynamics; tires; cameras; visual pattern recognition; measurement precision.

## 1. INTRODUCTION

Important efforts are being made in the automotive community to improve the performance of passenger cars, for example in terms of fuel consumption, comfort or stability. This needs an excellent knowledge of car behavior and more particularly of its lateral behavior in the domain of stability. The understanding of the vehicle's behavior requires to model it. Thus, different models have been developed over the last decades, each one having a certain level complexity in function of its domain of validity. A vehicle is a complex system. Consequently, a thorough comprehension requires a good modeling of the different subsystems which compose it. However, the understanding of the tire behavior, and more precisely the understanding of the transmission of the efforts between the tire and the road surface, is still limited. In consequence, if the vehicle modeling currently presents some limits, an improvement of the comprehension of the vehicle/road interface is primordial.

Even though the tire behavior is directly relative to the vehicle/road interaction, we are commonly interested in the interface between the wheel (rim + tire) and the ground. The understanding of this interface is based on the determination of the forces and the moments applied at the tire / road contact. Because of the measurement principle of the most dedicated industrial sensors, these data are determined near the wheel center. A lot of research has been made to model this interface as precisely as possible. The most known and the most commonly used model is the Pacejka's tire model (Pacejka and Bakker [1991]), which is based on the Magic Formula (MF). It is a semi-empiric model, which was already validated by the automotive community, for different types of solicitations - low or high vehicle lateral accelerations. That is why it is currently considered as a reference in the domain of tire modeling. Other frequently used models are the models of Guo (Guo and Ren [2000]) and Milliken (Milliken and Milliken [1995]), which are two hybrid models, or the model of knowledge of Zhou (Zhou et al. [1999]). An overview of the different most used tire models was made by Porcel (Porcel et al. [2001]). With these models and for a given adherence, the considered inputs are the longitudinal slip, the lateral tire slip angle, the normal charge and the camber angle. The generated forces and moments are considered as outputs. Recently, a new thermal and mechanical tire model, called TaMeTirE and developed by Michelin, was presented in Février and Fandard [2007]. Real tests have shown the advantage of the TaMeTirE model for tire forces prediction, in comparison with tire models based on the Magic Formula, and more particularly in the regions where the thermal effects are significant. As explained in Zami [2005], an accurate determination (measurement or estimation) of the inputs and the outputs is necessary, in order to improve the representation of the tire/road interaction by using one of these models. The presented works were made to improve the determination of one of the inputs: the camber angle.

This paper is organized as follows: in the second section, the camber angle is quickly defined. In a third section, the developed measurement principle is detailed. In a fourth part, the feasibility of the measurement method is validated and its measurement precision is evaluated from real tests with the laboratory test vehicle.

## 2. CAMBER ANGLE

### *2.1 Definitions*

There are different definitions of camber angle. Here it is defined as the angle between the external plan of the wheel and a plan perpendicular to the road - considered as a plan - as shown in Fig. 1. The camber is defined as positive when the top of the tire is outside the vehicle body and negative in the opposite case. This definition has been selected because the other existing definitions take the tire torsion phenomenon under lateral solicitations into account. Indeed, this phenomenon can not be currently determined in real-time.

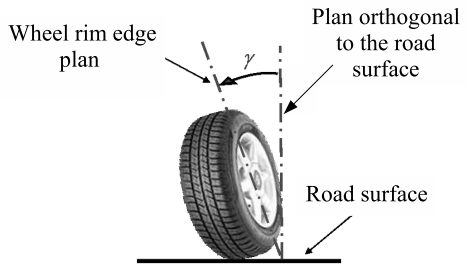


Fig. 1. Definition of the camber angle

### *2.2 Existing methods for camber determination*

Three major principles can be used to determine camber: the direct measurement, the indirect measurement or computation by measurement of other data and the use of maps issued from static tests. The three principles are detailed in the following subsections.

*Direct measurement* Camber can be directly measured with a dedicated sensor. In this case, the sensor unit is fixed in a plan parallel to wheel rim plan via a mechanical adapter. Such a system is commonly composed of two parts. The first part is fixed to the wheel hub via a collector ring, while the second is mounted on the vehicle body or the damper. This is in order to tolerate wheel cornering and damper deflections. When the sensor unit is fixed on the mechanical adapter, its displacements with respect to the road (and to car body) are the same as those of the wheel rim, despite the tire solicitations. Thus, the measured angle is the angle between the rim plan and the road, called wheel/road angle ($\gamma_{wheel/road}$). Once this angle is measured, the camber angle ($\gamma$) can be easily determined with the following relation (1):

$$\gamma = \gamma_{wheel/road} - 90^\circ \quad . \tag{1}$$

Fig. 2 shows the principle of camber direct measurement via 3 distance sensors. Many industrial sensors use this measurement principle. They differ by the precision of distance measurement and two distance sensors only can

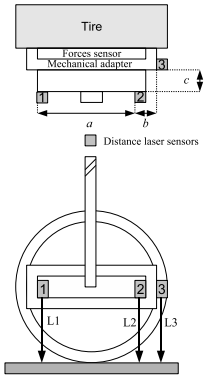


Fig. 2. Principle of camber direct measurement

be used. An application example is presented in Nüssle and Gnadler [2001]. A prototype sensor using 3 distance sensors was developed in the laboratory and results are presented in Basset et al. [2005].

$$\begin{aligned} L_{1\,2} &= (L_1 - L_2) * \left(\frac{a+b}{a}\right) \quad , \\ \gamma_{wheel/road} &= \arctan\left(\frac{L_3 - L_{1\,2}}{c}\right) \quad . \end{aligned} \tag{2}$$

*Indirect measurement* This method requires two different measurements. The first is the wheel/body angle ($\gamma_{wheel/body}$) measurement. That is done via a dedicated sensor, which is fixed in a plan parallel to the wheel rim as in the case of camber direct measurement. The second is the vehicle roll angle ($\theta$) measurement, which is the vehicle rotation around its longitudinal axle. Camber is then computed from the two measures with relation (3). An overview of different industrial sensors dedicated to camber indirect measurement is made in Basset et al. [2005].

$$\gamma = \gamma_{wheel/body} - \theta \quad . \tag{3}$$

*Computation method* This method consists in computing camber from different measures in the vehicle, which are:

- the rack displacement ;
- the damper deflection ;
- the lateral tire force.

As shown in Fig. 3, camber can be considered as the sum of two components: a kinematic camber and an elasto-kinematic camber. Both are determined from the above mentioned measures and two maps. The maps are issued from static measurements with the considered car. The kinematic map is determined by measurement of the (kinematic) wheel/body angle in function of the rack displacement and the damper deflection. The second map (elasto-kinematic map) is obtained by measurement of the same angle, while a lateral force is applied at the wheel center. During real tests, the real-time measurement of the three necessary parameters and the vehicle roll allows the real-time camber computation. Camber is simply the difference between the wheel/body angle and the vehicle roll. This method was studied in Zami [2005] and seemed to be really promising. It is currently used by different

carmakers. However, this approach is strictly reserved to carmakers or tire manufacturers because it requires specific test beds, which are very costly and dedicated to automotive fimrs. Additionally, the identification of the two maps must be done for each considered test car.

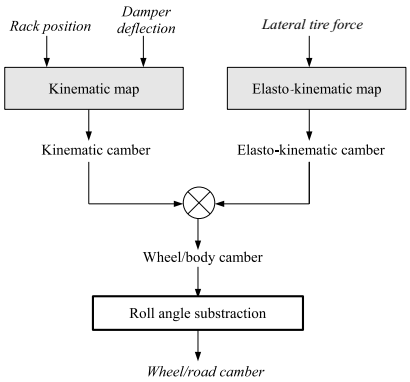


Fig. 3. Principle of camber computation

## 3. DEVELOPED DIRECT MEASUREMENT METHOD

The three methods presented have (their own) advantages and drawbacks. The major drawback of the direct and indirect measurement methods is their precision error, which is induced by the road unevenness, and their accuracy, which is dependent on the vehicle velocity. Our studies have shown that both solutions currently forbid to satisfy our needs in term of camber determination precision. From our experience, the camber computation solution seems to give good results in term of precision. However, it is reserved to carmakers, which is a major inconvenient in the domains of automotive modeling and automotive control. For these reasons, we chose to develop an innovative direct measurement method. The main goal was to reach our need in term of precision ($\pm 0.1°$) with no sensibility to the road unevenness and the vehicle velocity. The constraints that were defined in collaboration with a carmaker are the following:

- camber angle range: $\pm 10°$ ;
- tire deflection range: $\pm 10\,mm$ ;
- wheel steering range: full range ;
- data acquisition rate: 100 Hz ;
- camber measurement precision: $\pm 0.1°$ ;
- tire deflection measurement precision: $\pm 1\,mm$ ;
- bandwidth: 5 Hz.

### *3.1 Measurement principle*

*Projection of a laser pattern in front of the tire/road contact* A laser diode is fixed in a plan parallel to the wheel rim of the laboratory test car via a mechanical adapter, which was developed in the laboratory. The characteristics and the validity of the mentioned mechanical adapter were studied and presented in Lamy et al. [2007]. A diffraction lens is fixed in the head of the laser diode device in order to generate a laser pattern on the projection surface (road surface). While the laser diode is orthogonal to the projection surface, the laser pattern form is a rhombus. If the laser diode stays orthogonal to the projection surface (no rotation around the longitudinal axle of the tire), the increase of the distance with the test surface causes a homothetic increase of the pattern dimensions, and inversely (no variation of the pattern corner angles). In the same way, if the laser diode is rotated around the wheel longitudinal axle and the distance with the road surface does not change, the 4 pattern corner angles change. As long as the laser diode is only rotated around the wheel's vertical axle, the pattern is not deformed. In this case, there is only a displacement of the pattern with respect to the road surface. If the laser diode is subject to longitudinal or lateral displacements, the pattern displaces with respect to the road surface, but its parameters (angles, side lengths) do not change. Thus, it is possible to calculate the vertical displacement and the rotational angle of the laser diode (around the longitudinal axle of the wheel) at the same time. They can be determined from known values of pattern parameters (side length, corner angle, pattern displacement). In reality, the vertical displacement of the laser diode corresponds to the tire's normal deflection (in the axis system of the road), while its rotation around the wheel longitudinal axle corresponds to a variation of camber. In consequence, camber and tire deflection can be determined by a relation with known pattern characteristics. If such variables can be determined, it is possible to compute the camber and the tire deflection via a geometrical relation.

*Vision-based following of the pattern motion* The proposed method is based on the use of a camera, which is also fixed in a plan parallel to the wheel rim. Thus, in comparison with the laser diode, the camera positioning is not time variant, despite the wheel motion. If the characteristics and the positioning of the camera and the of laser diode are well chosen, the deformation of the laser pattern can be followed by the camera, while the wheel cornering, tire deflection and camber vary respectively in their full variation range. With this method, the measurement rate is equal to the used camera frame rate. The measurement precision is relative, first to the precision of determination of the used pattern characteristics, and secondly to the sensibility of the pattern deformation (variation of the used characteristics) with respect to the variations of camber and tire deflection. The measurement resolution is relative to the camera resolution (in pixels) and the resolution of the method used to determine the pattern parameters. Fig 4 shows an image acquired during a real test with the laboratory test car for a vehicle speed of 80 km/h.

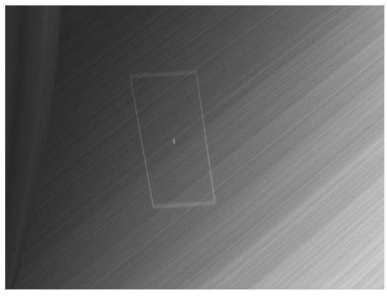

Fig. 4. Acquired image (real test at 80 km/h)

*Use of Hough Transform for pattern parameters determination* To determine the required pattern parameters, a solution is to detect the pattern lines in the images acquired with the camera. Once the lines are detected and reconstructed, the pattern corners can be deduced as their intersections. The knowledge of the position of the 4 corners in the image (in pixels) allows to calculate the lengths of the 4 pattern sides and the angles between two consecutive lines, which constitute the pattern. In the literature, many works concerning the extraction of lines and objects in digital images have been made over the last years. The most commonly used method is the extraction of straight lines based on the Hough Transform (HT) (Hough [1962] and Duda and Hart [1972]). An application of the HT is presented in Furukawa and Shinagawa [2003] and the results show its accuracy and its robustness to the image noise. Concerning the extraction of objects in images, an often used method is the approach of active contours based on Snakes (Kass and Terzopoulos [1988]). Both approaches have been tested in the laboratory in static tests via a test bed, which was developed in the laboratory. The camera images were acquired with industrial hardware and software, while two algorithms for the HT and the active contours method were implemented in the Matlab environment. The test results have shown that the HT-based solution was more appropriate to our needs in terms of computational cost and robustness to the image noise. In our context, the image noise is caused by the road texture and the ambient luminosity. An implementation of the HT in real-time is presented in Karabernou and Terranti [2005]. Thus, the method of lines extraction based on the Hough Transform was selected for our study. The acquired images were 256-gray level images. The methodology was to acquire images during real driving tests with the laboratory test, equipped with the laser diode and the camera. In post processing, we applied an adaptive threshold on each image, in function of Signal/Noise Rate (SNR). Here, the SNR is considered as the sum of the pixel amplitudes corresponding to the pattern, divided by the sum of the pixel amplitudes corresponding to the other pixels in the image. Results have shown that the developed method provides good results up to a certain level of SNR. There are two types of parameters decreasing the SNR: the lightest reflecting elements of the road (pixels with a high intensity in the image) and the ambient luminosity. Thus, while the ambient light is very high, the SNR is too low to detect the pattern lines efficiently. For this reason, the study of feasibility of our measurement method was performed in limited conditions, in term of amplitude of the ambient light. In these conditions, it was shown that the line extraction was very accurate, even when pixels corresponding to the lightest reflecting elements of the road surface were confounded with pixels corresponding to the pattern.

*Retained pattern parameters* For the computation camber ($\gamma$) and tire deflection ($\delta_{RD}$), two pattern parameters must be determined. The method principle is equivalent to solving a system of two geometrical equations, while the variables are $\gamma$ and $\delta_{RD}$. In order to obtain a measurement as accurate as possible, the selected pattern parameters must be the most sensible ones to variations of camber and tire deflection. To determine these two parameters, we developed a static test bed, which allowed to simulate variations of $\gamma$ and $RD$. We deduced that the parameters to be retained were the two pattern diagonals, called $D1$ and $D2$.

### *3.2 Computation of camber and tire deflection*

The method is composed of two steps. The first step is the determination of the used pattern parameters ($D1$ and $D2$) as functions of camber ($\gamma$) and tire deflection ($\Delta_{RD}$). More precisely, they are computed from the position and the orientation of the laser diode in comparison with the road (position and orientation in the road axis system). The computation is based on a geometrical function, detailed in the next subsection. The second step is the computation of $\gamma$ and $\Delta_{RD}$ from values of $D1$ and $D2$ in the camera images (respectively $D1_{pix}$ and $D2_{pix}$). The computation uses a homographic matrix, as explained in the second following subsection.

*Determination of the geometrical function: $F_g$* $D1$ and $D2$ can be determined from $\gamma$ and $RD$ with a geometrical function, called $F_g$. This function uses constant parameters, which are the position and the orientation of the laser diode in the wheel axis system and the aperture of the diffractive lens. The variables are $\gamma$ and $RD$. The value of the aperture was determined from static measurements (laser diode calibration). The determination accuracy of $D1$ and $D2$ is highly dependent on the determination accuracy of the laser diode position and orientation, and the lens aperture. Thus, the position and the orientation of the laser diode were measured via a very accurate tri-dimensional measurement machine, commonly used in the cutting-edge mechanical branch. The resolutions of measurements were 0.001 mm in positioning and 0.01° in orientation. Once the calibration of the laser diode is performed, the geometrical function Fg can be used to determine $D1$ and $D2$ from $\gamma$ and $RD$ (4):

$$(D1, D2) = F_g(\gamma, RD) \quad . \tag{4}$$

*Determination of the homographic matrix: H* Once the function $F_g$ is known, the second step of the method is to compute $D1_{pix}$ and $D2_pix$ via a homographic matrix, called $H$. This matrix is the product of two matrixes. The first matrix, called $A$ (3*3 matrix), is composed of constant parameters, which are the camera characteristics (focal, pixel size, etc.). The values of camera parameters are given by the camera manufacturer. These given values can not be used in our context because they are an approximation of the real values. The induced incertitude generates direct incertitude on the overall measurement results. Thus, the parameters were estimated via a camera calibration procedure, as it is often done in the domain of vision. A flexible camera calibration method is presented by Zhang (Zhang [2000]). The second matrix, called $RT$, is the product of two matrixes, $R$ and $T$ (respectively $3*3$ and $3*1$ matrixes), which respectively correspond to the orientation and the displacement of the camera (more precisely the camera axis system) with respect to the road (the road axis system). If the hypothesis of a flat road is made ($Z = 1$), the coordinates of the pixels corresponding to the laser pattern in the camera images ($U$ and $V$) are relative to the corresponding coordinates in the road axis system ($X$ and $Y$) from the equation (5).

$$\begin{bmatrix} U \\ V \\ 1 \end{bmatrix} = A * RT * \begin{bmatrix} X \\ Y \\ 1 \end{bmatrix} \quad , \tag{5}$$

$$\begin{bmatrix} D1_{pix} \\ D2_{pix} \\ 1 \end{bmatrix} = A * RT(\gamma, RD) * \begin{bmatrix} D1(\gamma, RD) \\ D2(\gamma, RD) \\ 1 \end{bmatrix} \quad . \tag{6}$$

$D1_{pix}$ and $D2_{pix}$ can be deduced by applying the Hough Transform on the images. The only two variables of the matrix $RT$ are the vertical translation ($T_Z$) and the rotation around the longitudinal axis of the road axis system ($R_X$). $T_Z$ and $R_X$ are respectively equal to the camber angle and the tire deflection in our context. In consequence, the matrix $RT$ can be considered as a function of $\gamma$ and $RD$, called $RT(\gamma, RD)$. As $D1$ and $D2$ are geometrical functions of ($\gamma$) and $RD$ ($F_{g1}(\gamma, RD)$ and $F_{g1}(\gamma, RD)$), $\gamma$ and $RD$ are the obtained by solving the first two equation of the following system of equations (6). The variations of $\gamma$ and $\Delta_{RD}$ with respect to $D1_{pix}$ and $D2_{pix}$ are represented in Fig. 5.

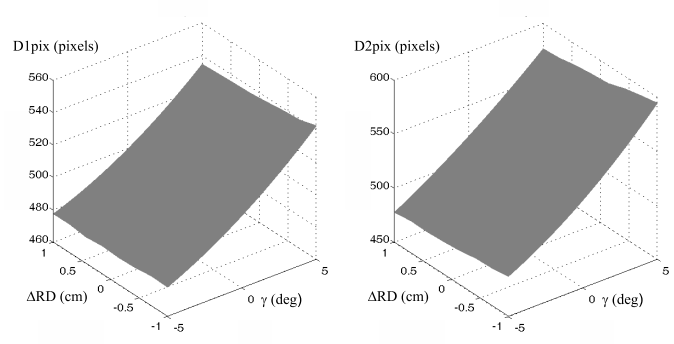


Fig. 5. Variations of $D1_{pix}$ and $D2_{pix}$ with $\gamma$ and $\Delta_{RD}$

## 4. FEASIBILITY STUDY AND MEASUREMENT PRECISION EVALUATION

### *4.1 Test environment*

*Hardware and software* To study the method feasibility and evaluate the measurement precision, we used a laser diode with a wavelength of 650 nm (red light) and a power of 30 mW. In order to have a SNR in the images as important as possible, the chosen camera is a Near Infrared (NIR) camera. Indeed, such a camera has an integrated light band-pass filter around 640 nm. The filtering allows the degradation of the amplitude of the pixels, which do not correspond to the laser pattern in the image. The used camera was a high-resolution CCD camera [1] (1392 (H) * 1040 (V) pixels). For reasons of cost, the camera frame rate was only 30 Hz, which is lower than the desired rate of 100 Hz. However, that was sufficient in the context of feasibility study because the maximal characteristic frequency of camber dynamics is near 5 Hz. The evaluation of the proposed method was made in post processing in the Matlab environment by using a classical personal computer (PC). The acquisition of the camera images was performed via a classical image acquisition card, integrated in the PC.

[1] http://www.subtechnique.com/pulnix/PDFs/tm1400.pdf

*Overall computational cost* The image processing and the computation of camber and tire deflection were performed once the images were acquired during real tests with the laboratory test car. As already mentioned in the paper, we developed an algorithm for the HT implementation. The solving of the system of the first two equations in (6) was made via a genetic algorithm, which we developed. The use of such a solving approach was necessary because of the high complexity and the non linearity of the equations. In order to have a computational cost as low as possible, the developed algorithm was based on the Simplex (Ren et al. [2007]). Because we have an a priori on the initial values of camber and tire deflection, the research spaces of the two variables ($\gamma$ and $\Delta_{RD}$) were very low. In spite of the inappropriate environment for such a problem (Matlab environment), the computational cost for the extraction of the lines in the images and the calculation of $D1_{pix}$ and $D2_{pix}$ was evaluated to 1 second. The computational cost of the genetic algorithm convergence was also lower than 1 second. Thus, the overall computational cost was evaluated to 2 seconds, that is clearly sufficient in a post processing context.

### *4.2 Test protocole*

The tests were performed in day light with a classical ambient light (not determined). The test vehicle followed a straight trajectory with different constant speeds (20, 40, 60, 80 and 100 km/h). The camera and the laser diode were fixed on a parallel plan to the rim plan of the front left wheel via the mechanical adapter. The test track was a flat road with a classical granularity, with unevenness up to 1 cm. The test car driver endeavored to keep a straight line trajectory and a constant velocity. Once the vehicle has reached its consign speed, the variations of damper deflection and wheel cornering are very low. In consequence, the lateral and vertical forces at the wheel/road contact can be considered constant. Thus, we can make the hypothesis that the variations of tire deflection and both kinematic and elasto-kinematic components of camber are equal to zero during the quasi static phase (constant vehicle speed).

### *4.3 Test results*

The principle of evaluation of the measurement precision for camber and tire deflection consists in calculating the fluctuations of the two above mentioned measures around their mean value in quasi static state. The selected value was the standard deviation of the measures ($3\,\sigma$). The tests have shown the robustness of the proposed method to the road unevenness. Indeed, when the vehicle starts moving, the road texture becomes a flow in the images, while the laser pattern sides are not deformed and can be really considered as straight lines. We evaluated that the pattern is not deformed by the road unevenness for vehicle speeds higher than 0.5 km/h. Fig. 6 shows an image acquired for a vehicle velocity of 80 km/h. In the image, we can see the reconstruction of the detected pattern lines after application of the Hough Transform. In the same way, we confirmed the validity of the developed mechanical adapter, in term of robustness to mechanical vibrations and to the caster angle. Indeed, the displacement of the laser pattern in the images was very low for all our

tests. Therefore, the mean value of the measured camber and tire deflection could be considered as a measurement reference. The calculated standard deviations ($3\,\sigma$) for the two corresponding measures have shown very promising results. The measurement precisions were evaluated at $\pm\,0.2°$ for camber angle and $\pm\,1\,mm$ for tire deflection.

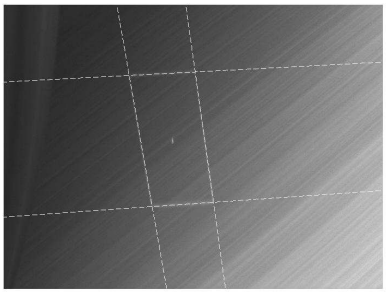

Fig. 6. Application of HT (real test at 80 km/h)

## 5. CONCLUSION

### *5.1 Conclusions on the presented study*

In this paper, a new vision-based method for camber direct determination was presented. This approach allows to measure tire deflection simultaneously. First, existing solutions for camber determination were mentioned, and their advantages and drawbacks were given. In order to validate the robustness of the new developed method to the road unevenness, and to evaluate its measurement precision, a measurement prototype was developed. Real tests were carried out with the laboratory test car. In a context of feasibility study, the determination of camber and tire deflection was made in post processing. Test results allowed to evaluate a measurement precision of $\pm\,0.2°$ for camber and $\pm\,1\,mm$ for tire deflection. Thus, we can conclude that the results of the presented study are really promising in comparison with the desired measurement performances, which were defined in collaboration with a carmaker.

### *5.2 Outlook*

For reasons of cost, the preliminary tests were carried out by using a camera with a frame rate of 30 Hz (instead of the 100 Hz desired) and a laser diode with a light power of 30 mW. Further works will be performed by using a camera with a frame rate of 100 Hz and a laser diode with a higher power. Under these conditions, the measurement sensibility to the ambient light (which decreases the SNR) and the data rate should be improved. The main purpose of further works is to develop an adaptive image processing, in order to reach the desired measurement precision of $\pm\,0.1°$. At the same time, more adapted hardware and software will be used to decrease the overall computational cost in a real-time context.

## ACKNOWLEDGEMENTS

We would like to thank the Research Department of Renault for its collaboration and contribution to this study with the loan of test tracks in Aubevoye (France) and the possibility to carry out tests with a test car driver.

## REFERENCES

M. Basset, G. Girardin, and G. L. Gissinger. Direct camber angle measurement using distance sensors. In *European Congress on Sensors & Actuators for Advanced Automotive Applications*, 2005.

R. O. Duda and P. E. Hart. Use of the hough transformation to detect lines and curves in pictures. *Communications of the ACM*, 15:11–15, January 1972.

P. Février and G. Fandard. A new thermal and mechanical tire model for handling simulation. In *14th Conference on Vehicles Dynamics*, June 2007.

Y. Furukawa and Y. Shinagawa. Accurate and robust line segment extraction by analyzing distribution around peaks in hough space. *Computer Vision and Image Understanding*, 92:1–25, 2003.

K. Guo and L. Ren. A non-steady and non-linear tire model under large lateral slip condition. *SAE Transactions*, 2000.

P. Hough. Methods and means for recognizing patterns. U. S. patent 3, 069,654, December 1962.

S. M. Karabernou and F. Terranti. Real-time fpga implementation of hough transform using gradient and cordic algorithm. *Image and Vision Computing*, 23:1009–1017, 2005.

M. Kass and A. Witkin D. Terzopoulos. Snakes: Active contour models. *International Journal of Computer Vision*, 55:321–331, 1988.

C. Lamy, J. Caroux, M. Basset, J. L. Gissinger, P. Romieu, and D. Poli. Comparison of optical and gps/ins based tire slip angle estimation. In *5th IFAC Symposium on Advances in Automotive Control*, 2007.

W.F. Milliken and D.L. Milliken. *Race car vehicle dynamics.* SAE Publication, 1995.

M. Nüssle and R. Gnadler. Measuring equipment for the evaluation of tyre characteristics under real driving conditions. *ATZ*, 103:13–16, 2001.

H. Pacejka and E. Bakker. The magic formula tyre model. In *Int. Colloq on Tyre models for Vehicle Dynamics Analysis*, pages 1–18, 1991.

A. Porcel, P. Laurence, M. Basset, and G. L. Gissinger. Tyre model for vehicle simulation: overview and real time solution for critical situations. In *IEEE International Conference on Control Applications*, 2001.

Z. W. Ren, Y. San, and J. F. Chen. Hybrid simplex-improved genetic algorithm for global numerical optimization. *ACTA AUTOMATICA SINICA*, 33, 2007.

B. Zami. *Contribution à l'identification de la liaison véhicule/sol d'un véhicule automobile. Estimation des paramètres de modèles de pneumatiques.* PhD thesis, Université de Haute Alsace, 2005.

Z. Zhang. A flexible new technique for camera calibration. *IEEE Transactions on Pattern Analysis and Machine Intelligence*, 22(11):1330–1334, 2000.

J. Zhou, J. Y. Wong, and R. S. Sharp. A multi-spoke, three plane tyre model for simulation of transient behavior. In *Vehicle System Dynamics*, volume 31, pages 35–45, 1999.